Available online at www.sciencedirect.com
SCIENCE DIRECT®
Journal of Molecular Catalysis B: Enzymatic 22 (2003) 119–133
JOURNAL OF MOLECULAR CATALYSIS B: ENZYMATIC
www.elsevier.com/locate/molcatb

Preparation and properties of lipase immobilized on MCM-36 support

Emil Dumitriu [a,*], Francesco Secundo [b], Joël Patarin [c], Ioana Fechete [a]

[a] *Laboratory of Catalysis, Technical University of Iasi, 71 D. Mangeron, Iasi 6600, Romania*
[b] *Istituto di Chimica del Riconoscimento Molecolare, v. Mario Bianco 9, 20131 Milan, Italy*
[c] *Laboratoire de Matériaux Minéraux, Université de Haute Alsace, 3 rue Alfred Werner, 68093 Mulhouse, France*

Received 30 January 2003; accepted 30 January 2003

Abstract

Based on pure MCM-22 precursor, MCM-36 was produced by swelling and pillaring with SiO_2 pillars. These materials were characterized by X-ray diffraction (XRD), scanning electron microscopy (SEM), thermogravimetric analysis/differential scanning calorimetry (TGA/DSC), MAS NMR, and N_2 adsorption isotherms. Compared with the MCM-22 sample, the resulting MCM-36 material contains a mesoporous region between the microporous layers, with a mesopore volume of 0.472 cm^3/g, and the surface area increased up to 671 m^2/g. Lipase from *Candida antarctica* B (CALB) was immobilized on both supports by physical adsorption at equilibrium. Twenty milligrams of CALB/g of MCM-22 was adsorbed on the external surface of crystals, while only 4 mg CALB/g support was adsorbed onto the mesoporous hybrid material MCM-36. The mechanism of adsorption was also discussed. The acylation of alcohols (1-butanol and 1-octanol) by vinyl esters (vinyl acetate and vinyl stearate) was used as a test reaction in order to evaluate the catalytic activity of MCM-36-immobilized lipase. The test reaction indicated MCM-36-immobilized enzyme as an active catalyst for the acylation and its activity was approximately two times higher than that of the free lipase (for the vinyl acetate/1-butanol system).

Keywords: Enzyme immobilization; Lipase; Acylation; MCM-22 zeolite; MCM-36

1. Introduction

A distinguishing feature of the recent developments in organic synthesis is an emphasis upon the selectivity. At the same time, in the last years the control of stereochemistry, and in particular the formation of only one optical isomer (enantioselectivity), is one of the most active areas of research because of its prime importance in the synthesis of fine chemicals, mainly for pharmaceutical and agrochemical products. The experimental data indicated enzymes as very attractive and useful catalysts for both purposes, because enzymes can accept and transform selectively not only natural substrates but also foreign synthetic substrates in both aqueous solutions and organic solvents under mild conditions.

Among hydrolases, the lipases are often used because they are inexpensive and easy to handle for synthetic organic chemists. Other reasons for the enormous interest with regard to the use of lipases as biocatalysts include: (i) they are stable in organic solvents, (ii) do not require cofactors, (iii) possess broad substrate specificity, (iv) exhibit a high enantioselectivity [1]. The biological function of lipases is to catalyze

* Corresponding author. Tel.: +40-232-278-683; fax: +40-232-271-311.
E-mail address: edumitri@ch.tuiasi.ro (E. Dumitriu).

1381-1177/03/$ – see front matter © 2003 Elsevier Science B.V. All rights reserved.
doi:10.1016/S1381-1177(03)00015-8

the hydrolysis of esters, but as proved in vitro they are also able of catalyzing the reverse reaction, achieving esterification, transesterification (acidolysis, interesterification, alcoholysis), aminolysis, oximolysis and thiotransesterification [1–4] in various solvents. More than 50 lipases have been identified, separated, purified and characterized until now [5], which originate in such natural sources as plants, animals and microorganisms. Lipase B from *Candida antarctica* (CALB), which was the subject of our study, is one of the most popular lipases used in organic synthesis.

Lipases have been used frequently in the form of a crude protein extract as catalysts for various reactions. However, the use of crude lipases often leads to a longer time and/or a lower enantioselectivity and even it may cause the opposite selectivity due to the presence of several contaminating enzymes [6]. Therefore, the use of pure enzymes is recommended. In order to use lipases more economically and efficiently immobilization techniques can be applied. For instance, the immobilization with hydrophobic silica matrices was applicable to lipases from different sources, and the activity of immobilized lipases was higher than that of the commercially available crude enzymes [7]. On the other hand, immobilization of enzymes greatly reduced the economic difficulties associated with biocatalysis: the productivity of the biocatalytic process increased by concentrating the catalyst on the reactional media, it ensured the reusability of immobilized lipase and minimized the cost of product isolation, it provided operational flexibility, and the immobilization also increased enzyme thermal and chemical stability. Many immobilization techniques have been reported, using synthetic polymers [8–11] or natural polymeric derivatives [12,13], inorganic materials like diatomaceous earth (Celite) [14–16], controlled-pore glasses [17], silica [16], zeolites [18–29], phyllosilicates [30], mesostructured oxides [31–34], layered double hydroxides [35], ceramics [36], inorganic matrices based on sol–gel processes [7,37,38] and microemulsion-based gels [39].

On the other hand, immobilization of enzymes by physical procedures such as adsorption on a solid is very attractive because of its simplicity. In this context, the use of zeolitic materials is of great interest. The zeolites and related materials have potentially interesting properties, such as large surface area (between 200 and $\sim$1000 m^2/g), hydrophobic or hydrophilic behavior, and electrostatic interactions, with the possibility of different ion-exchanged forms, mechanical and chemical resistance. Additional advantages could be mentioned as their ease of water dispersion/recuperation, as well as the high water uptake capacity. Therefore, the compositional and structural variances of molecular sieves offer a powerful tool for tuning the carrier properties. The main drawback of zeolites consists in their small pore sizes, viz. the enzyme cannot enter the inner channels of the zeolite matrix. Later, this inconvenience was surpassed by the synthesis of mesoporous materials like MCM-41, FSM-16 or SBA-15. As a consequence, the immobilization of different enzymes as lipase [18,23], acid phosphatase [19], cutinase [20,24,26,27], glucose oxidase [22], α-chymotripsin and thermolysin [25], tyrosinase [28], penicillin acylase [33], subtilisin [34], cytochrome *c*, papain, trypsin and peroxidase [31,32,34] on such micro- and mesoporous materials was reported. Current literature, however, suffers from lack of systematic approach to lipase immobilization on zeolitic materials. As can be seen, few reports are exclusively dedicated to the lipase immobilization on zeolites and related materials.

Another interesting approach in this area consists in the use of lamellar zeolite precursors that are pillared with suitable pillars in order to create a large surface area and mesopores, which will favor the immobilization of enzymes. This is the case of the MCM-36 material, which is obtained by SiO_2-pillaring of the MCM-22 precursor. To our knowledge, the use of MCM-36 as a support for enzymes immobilization has not been reported previously, whereas the MCM-22 zeolite was only used for the immobilization of proteases [29].

This paper presents our investigations on the synthesis of pure MCM-36, a hybrid solid which comprise two components: alternate layers of microporous zeolite and silica pillars creating mesoporous domains, and on its application as carrier for CALB. The new enzyme-supported material was tested as biocatalyst for the alcoholysis of two vinyl esters.

2. Experimental

2.1. Synthesis of the support (MCM-36)

The hydrothermal synthesis of the layered aluminosilicate MCM-22 precursor (MCM-22(P)) was

carried out by using hexamethyleneimine (HMI, 99%, Aldrich) as organic template, SiO_2 (Aerosil, Degussa), $NaAlO_2$ (56% Al_2O_3, 37% Na_2O, Carlo Erba), NaOH (98%, Prolabo) and deionized water. Based on the synthesis procedures previously reported [40–42], a typical sample with Si/Al = 50 was prepared as follows. Sodium aluminate (0.24 g) and sodium hydroxide (0.80 g) were dissolved in 103.45 g of deionized water. Then, 7.5 g of SiO_2 were added to this solution under stirring. After 30 min of stirring, the resulting gel was introduced into a 100 ml Teflon-lined stainless-steel autoclave which was then rotated at 60 rpm, and heated at 415 K for 195 h. After quenching the autoclave in cold water, the sample was filtered, washed thoroughly with deionized water until a pH lower than 9.0 was reached. Several experiments using different sources of silicon and aluminum were performed.

MCM-36 was prepared according to the method previously reported [40]. The wet cake obtained as above (25–30% solids) was mixed with cetyltrimethylammonium chloride (CTMAC, 25%, Aldrich) and tetrapropylammonium hydroxide (TPAOH, Aldrich) with a relative weight ratio of 1:4:1.2 (MCM-22 precursor/CTMAC/TPAOH). The pH of the solution was adjusted to 13.5 and the mixture placed in a three-neck-round bottomed flask, fitted with stirrer, thermometer and reflux condenser. The mixture was hold at 353 K for 68 h and at room temperature for 4 h under continuous stirring. The resulting swollen material was filtered and washed with a small amount of distilled water, and dried at room temperature. Tetraethyl orthosilicate was added as pillaring agent to the swollen MCM-22 precursor with a relative weight ratio of 5:1 (MCM-22(P)/TEOS). The mixture was heated at 353 K for 25 h in a nitrogen atmosphere under continuous stirring, and then the solid material was recovered by filtration and dried overnight. The resulting solid was hydrolyzed in water with a 1:10 ratio (w/w, solid/water) at 413 K for 6 h, and then filtered and dried at 300 K overnight. During the hydrolysis, the pH of the mixture was adjusted at 1.92 with 1 M HNO_3. Finally, the sample was heated at 723 K for 3 h in nitrogen and at 812 K for 6 h in air (heating rate of 2 K/min).

The calcined zeolitic material was ion-exchanged with an excess of 1 M aqueous NH_4NO_3 (liquid-to-solid ratio of 10 cm^3/g) and stirred continuously at 353 K for 8 h. This procedure was repeated for three times. After filtering and drying, the resulting NH_4^+MCM-36 was calcined at 773 K for 5 h in air to form H–MCM-36.

The resulting zeolitic materials were characterized by various techniques. Powder X-ray diffraction (XRD) patterns were collected to estimate crystallinities and structural types of the synthesized materials on a Philips PW 1800 diffractometer (Cu Kα radiation, variable slit openings), as well as on a STOE STADI-P diffractometer equipped with a curved germanium primary monochromator and a linear position-sensitive detector, using Cu Kα1 radiation. Data were collected in the 2θ range from 0.0 to 50°. The morphologies and crystal sizes of the synthesized specimens were examined by scanning electron microscopy (SEM) on a PHILIPS XL30 apparatus.

Solid state ^{29}Si and ^{27}Al MAS NMR spectra were obtained on a Bruker MSL-300 spectrometer. The samples were placed in 7 mm zirconia rotors (rotation speed = 5 kHz) and analyzed at resonance frequencies of 78.2 MHz for ^{27}Al and 59.6 MHz for ^{29}Si. The corresponding acquisition times were 0.172 and 0.049 s, respectively. The recycle delays were 3 s for ^{29}Si and 0.5 s for ^{27}Al, respectively. The chemical shifts were referenced to tetramethylsilane for silicon and to 1 M aqueous acidic $Al(NO_3)_3$ for aluminum, as external standards.

Thermal analysis (thermogravimetric analysis/differential scanning calorimetry, TGA/DSC) of the as-synthesized samples was performed on a SETARAM TG 111 system. The analyses were carried out in a nitrogen atmosphere in the temperature range 298–1073 K with a heating rate of 5 K/min.

The nitrogen adsorption measurements were carried out at 77 K with a Micromeritics ASAP 2100 system. The samples were degassed at 573 K and 10^{-3} Pa for 24 h prior to the adsorption measurements. The specific surface areas were determined by the BET method. The micro- and mesopore size distributions were obtained from the adsorption branch of the isotherms. The pore volume and the average diameter of the pores were calculated by using *t*-plots.

2.2. Immobilization of lipase on MCM-36

Candida antarctica lipase B was initially purified from Chirazyme L-2 (Boehring Mannheim) following a procedure described elsewhere [43].

Immobilization of lipase by "adsorption" was carried out using 2 mg of purified lipase dissolved in 2 ml of 0.1 M phosphate buffer (pH 7) to which was added the MCM-36 support (200 mg). The mixture was gently stirred for 3 h at room temperature. The resulting lipase-supported MCM-36 or MCM-22 was centrifuged, washed several times with the same buffer solution and then dried under vacuum (0.02 mbar, 30 °C, 20 h). After the third washing the residual water did not exhibit any enzymatic activity in the hydrolysis of *p*-nitrophenyl laurate (0.1 ml of a 3 mg/ml solution in 2-propanol) in 0.02 M potassium phosphate buffer, pH 7 (0.9 ml). The samples as obtained were labeled as MCM-36/pa and MCM-22/pa (pa = physically adsorbed), respectively. The enzyme content of the filtrate solution was determined by measuring the protein concentration by Bradford's method using Bio-Rad kit.

Immobilization of lipase by "deposition" on MCM-36 was carried out as follows. Aliquots of a 0.5 mg/ml solution of purified lipase in 0.1 M potassium phosphate buffer (pH 7) were diluted with the same buffer to 1.4 ml and added to different samples (each containing 50 mg) of MCM-36 to obtain a final lipase/support loading of 0.625, 1.25, 2.5, 5, 8, 11 and 15.5 mg/g. The obtained slurry was stirred at room temperature for 3 h, and then the water was removed by vacuum (0.02 mbar, 30 °C, 20 h).

2.3. Determination of the catalytic activity of immobilized lipase

To avoid possible drying or hydrating effects of the zeolites the immobilized lipases, the organic solvent (toluene) and the reactants (1-butanol, 1-octanol, vinyl acetate and vinyl stearate) were separately pre-equilibrated to the same water activity before starting the reaction. This was done by equilibration in sealed containers for 24 h at 25 °C against molecular sieves (NaA), $a_w < 0.1$.

For the alcoholysis runs, in a typical experiment immobilized lipase (10 mg), toluene (870 μl), vinyl acetate (100 μl, 1.085 mmol) and 1-butanol (30 μl, 0.328 mmol) were placed in a 10 ml screw-capped vial and shaken at 150 shots per min. At different times, aliquots were withdrawn from the reaction mixture and analyzed by GC (HP-1 crosslinked methyl silicone gum, 20 m). The conditions of analysis were: oven temperature from 308 to 453 K with a heating rate of 15 K/min, H_2 as carrier gas.

3. Results and discussion

3.1. Synthesis and characterization of support

The first data concerning the synthesis of MCM-22 have been reported by Mobil workers in 1990 [44]. The structure of MCM-22 has been shown to consist of layers linked together along the *c*-axis by oxygen bridges and contains two independent pore systems [45,46]. Within the layers are two-dimensional sinusoidal 10 M ring channels, and between two adjacent layers are 12 M ring supercages (~0.71 nm × 0.71 nm × 1.82 nm) communicating with each other through 10 M ring apertures. The unusual structure of zeolite MCM-22 is formed from a layered precursor designated as MCM-22(P) [44], which is able to condensate the silanol groups present on the layer surfaces by calcination, leading to the 3D structure as shown in Fig. 1. This precursor has been also used as starting material to prepare the pillared structure known as MCM-36.

In our study, we used the lipase adsorption at equilibrium as technique of immobilization, because it provides more accurate information on the enzyme–support interactions. Therefore, the selection of a suitable support must be preceded by characterization studies that yield fundamental information on the solid and surface properties. Consequently, various techniques of investigation were applied in order to characterize both the MCM-22(P) phases and the final support that will be used for lipase immobilization.

The crystallization of synthesis mixtures with SiO_2/Al_2O_3 ratios of 30, 50 and 100 were investigated. The sample obtained from the synthesis mixture with the SiO_2/Al_2O_3 ratio of 100 is pure MCM-22(P). The diffraction pattern of this sample (Fig. 2) agrees well with those previously reported (e.g. [47]). The calcined sample gives sharper reflections than the as-synthesized sample, as shown in Fig. 2b, and the (0 0 1) reflection characteristic of the layered structure of MCM-22(P) disappeared. The high crystallinity and phase purity of the MCM-22 zeolite could be considered as proof for the quality of its precursor.

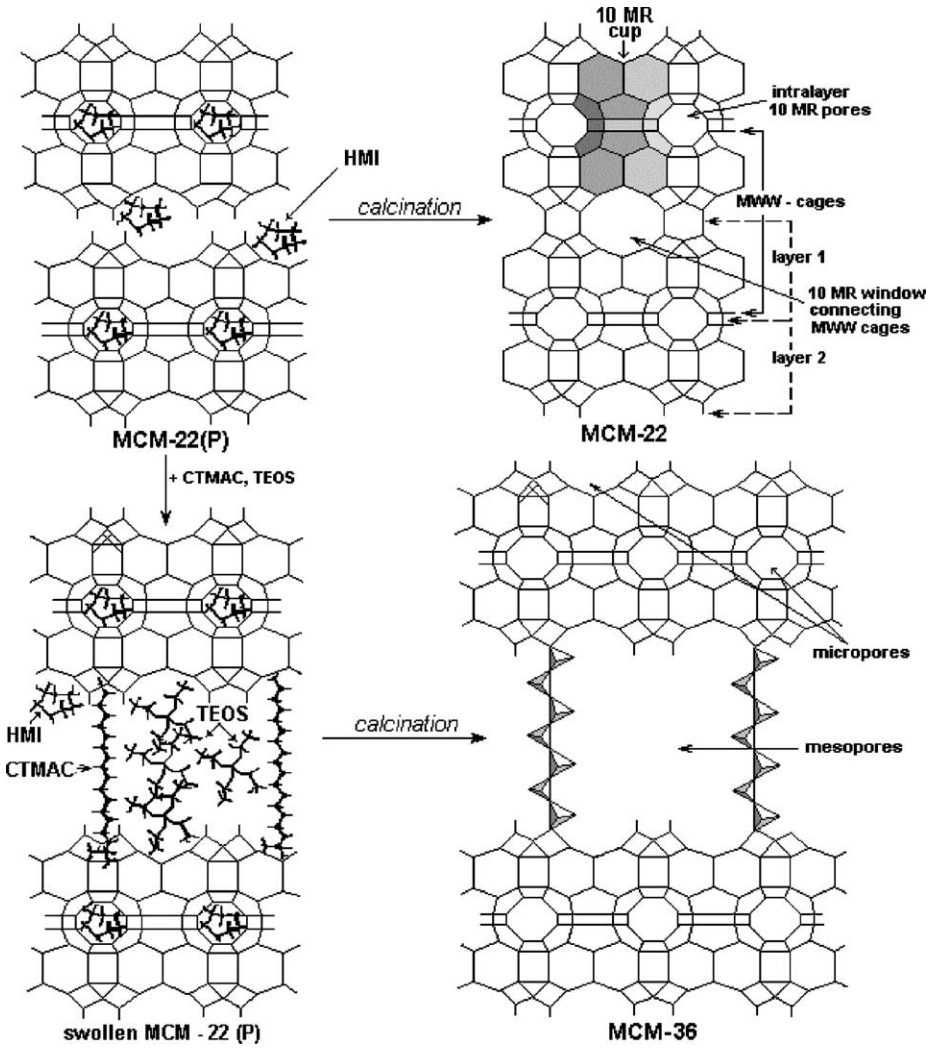

Fig. 1. Schematic presentation of the MCM-22(P), MCM-22 and MCM-36 structures.

The morphology of the MCM-22(P) sample is shown in Fig. 3a. The samples have a platelet or platelet-like morphology with a diameter of about 2–5 μm and 0.05–0.1 μm thickness. Some large particles are formed by the aggregation of these platelets. The crystals of MCM-22 possess similar morphology.

By contrast, MCM-36 shows larger agglomerated crystallites with diameters varying from 2 to 7 μm, while the distinctive platelet structure has disappeared completely (see Fig. 3b). He et al. [48] attributed this change of morphology to the silica pillars between layers of swollen MCM-22 resulting in at least doubling of the platelet thickness.

Since during the zeolite synthesis and/or the calcination process, some extra-framework aluminum species could appear, MAS NMR analysis was performed in order to provide structural information on the three materials: MCM-22(P), MCM-22 and MCM-36. The ^{29}Si and ^{27}Al MAS NMR spectra are shown in Fig. 4.

^{29}Si MAS NMR analyses on MCM-22 evidenced the presence of at least seven peaks, the most important ones about −105.2, −110.9, −113.3, −116.0 and

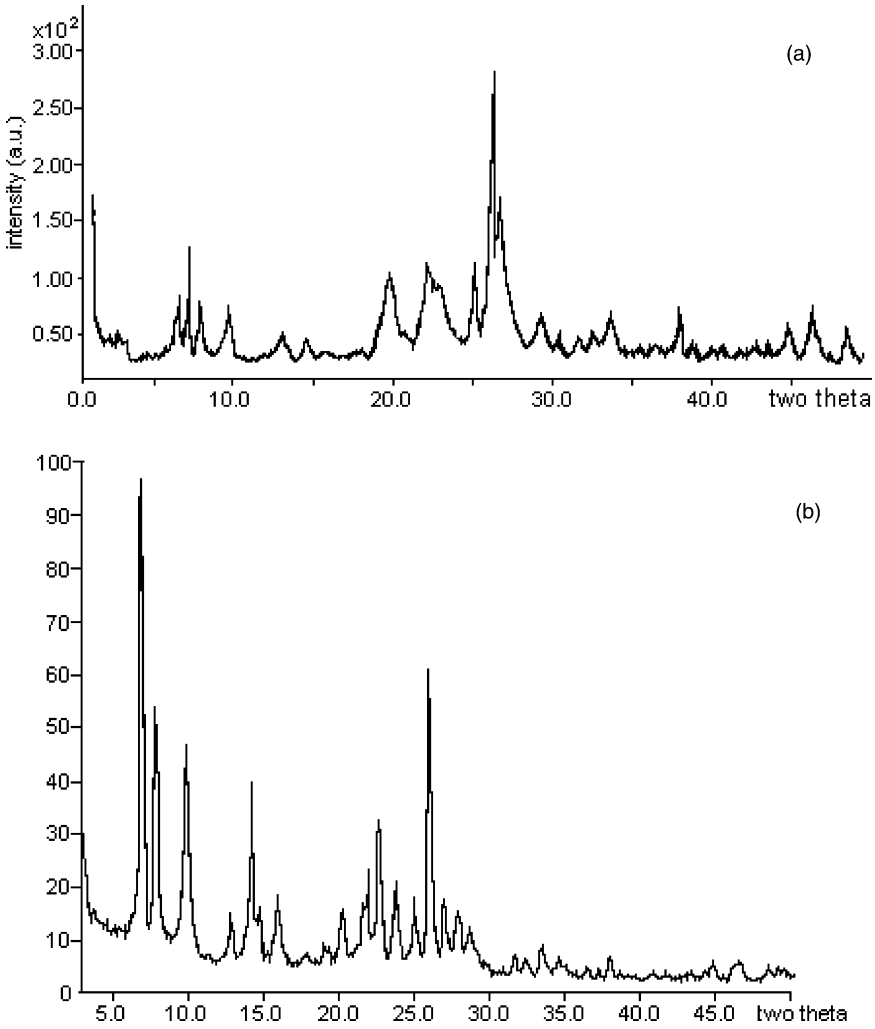

Fig. 2. Powder XRD patterns of: (a) the MCM-22(P) sample and (b) the calcined sample (MCM-22) synthesized from the mixture with a SiO_2/Al_2O_3 molar ratio of 100.

−119.8 ppm. These resonances result from the combined effects of crystallographic site non-equivalence and the number of nearest neighbor aluminum atoms on the ^{29}Si chemical shifts [49].

The ^{27}Al MAS NMR spectrum of MCM-22(P) shows a signal with a maximum at 55.4 ppm and a shoulder at 49.7 ppm, corresponding to two out of three different tetrahedral framework aluminum species [47]. In MCM-22, the presence of three different framework species is due to the preferred incorporation of the aluminum atoms into some specific sites [49,50]. The resonance at 49.2 ppm has been assigned to the aluminum sites on the external and/or large cavities [50]. Upon calcination, an additional peak is observed at 1.3 ppm, which results from the presence of extra-framework aluminum species. For MCM-36 this peak is less intense, indicating that aluminum cations are more stable in the zeolite layers of MCM-36 than those of MCM-22.

The formation of the 3D structure of MCM-36 was verified applying various techniques. Firstly, the X-ray diffraction pattern was recorded to check the

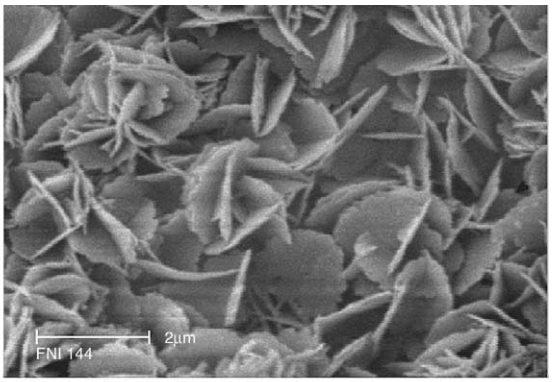

(a)

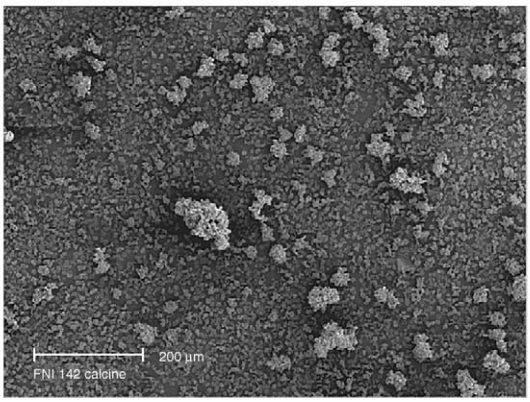

(b)

Fig. 3. Scanning electron micrographs of the MCM-22(P) sample synthesized from a mixture with SiO_2/Al_2O_3 molar ratio of 100 (a), and the pillared structure MCM-36 (b).

formation of the MCM-36 phase. The XRD pattern of the MCM-36 sample is shown in Fig. 5. All peaks observed correspond perfectly to those of the MCM-36 material reported previously [34,36].

Compared with the pattern of MCM-22(P) in Fig. 2, the characteristic 0 0 2 reflection at $2\theta - 6.6^\circ$ disappears upon pillaring (Fig. 5). On the other hand, an intense low-angle reflection appears at 2θ between 1 and 2°, which corresponds to a *d*-spacing of 5.9 nm. This represents the new *c*-parameter of the unit cell. The *d*-value includes both the *c*-parameters of the unit cell of MCM-22 and the spacing distance between the layers of MCM-36. Therefore, the distance between two layers in MCM-36 can be calculated by subtracting the thickness of the layer (*c*-parameter of MCM-22 is equal to 2.51 nm [45]). The values for the obtained sample suggest an average interlayer distance of 3.4 nm.

The formation of a new structure (MCM-36) from MCM-22 precursor is also proved by TGA/DSC curves (Fig. 6). With MCM-36, the weight loss (∼23%) in the first step (473–743 K) is much higher than that for MCM-22 (∼11%). This weight loss is attributed to the removal of the organic swelling agent from the zeolitic structure. By contrast, the mass loss (∼8%) above 743 K is rather similar to that (∼7%) for MCM-22.

The textural properties of the calcined MCM-22 and MCM-36 samples were measured by nitrogen adsorption. The pure MCM-22 sample has a specific surface area of 465 m^2/g and a total pore volume of 0.284 cm^3/g, which are typical for this type of zeolite [51]. The specific area of the MCM-36 (671 m^2/g) sample is higher than that of MCM-22. The total pore volume is also higher for MCM-36 than for MCM-22, and an important contribution of a mesopore volume was established.

Fig. 7 shows N_2 adsorption/desorption isotherms of the MCM-22 and MCM-36 samples. This figure clearly evidences the difference between the two materials. Thus, in the case of MCM-22 about 80% of its sorption capacity is already used at a low relative pressure ($p/p_0 < 0.1$), due to the zeolite micropores. In the case of the MCM-36 sample, the noticeable increase of the adsorption capacity up to $p/p_0 = 0.4$ could indicate condensation in mesopores.

Further, the pore volume and the external surface areas were estimated by using *t*-plots. It was found for the pillared structure of MCM-36 has a mesopores volume of 0.472 cm^3/g, and the surface area in the mesopores was estimated to about 61.9 m^2/g. An average mesopore size of approximately 31 Å was finally estimated, and this value satisfactorily agrees with the XRD data. As a conclusion, a mesopore region with ∼34 Å thickness between the microporous layers was identified. It is worthwhile to note that the pore structure of the MCM-22 layers stays intact during the swelling and pillaring process as previously proved by the sorption characteristics of linear alkanes [48].

3.2. Immobilization of CALB on MCM-22 and MCM-36

The immobilization of enzymes onto high surface area of supports by physical adsorption is one of the simplest methods of immobilization with the added

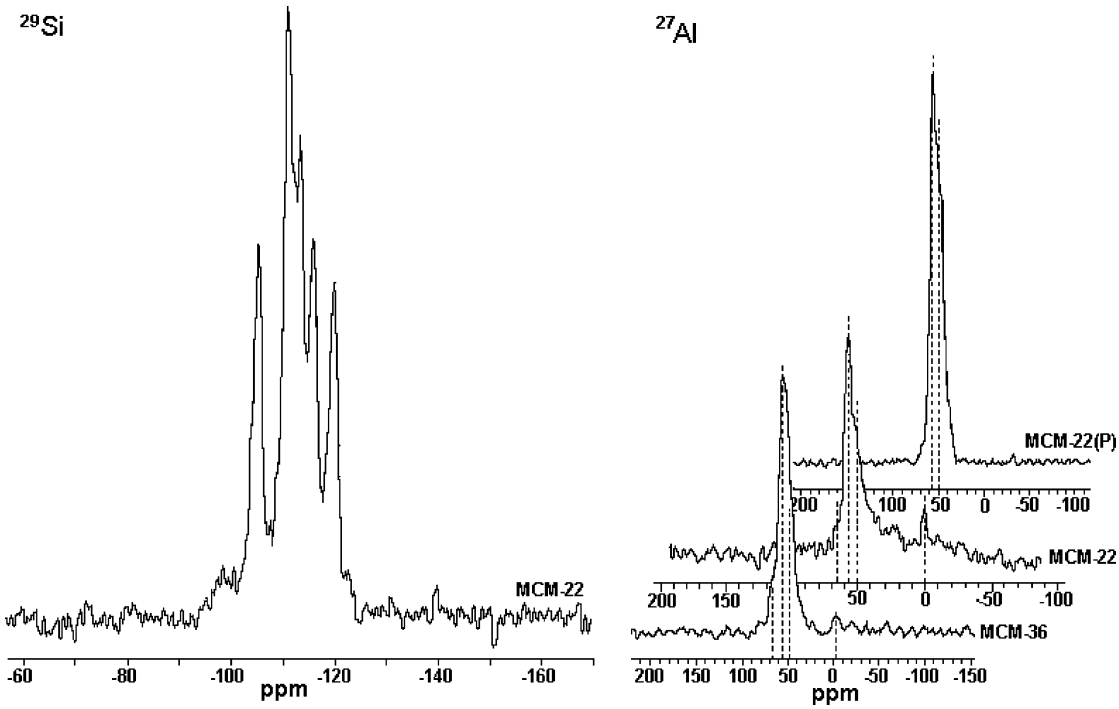

Fig. 4. MAS NMR spectra of MCM-22 and MCM-36 samples.

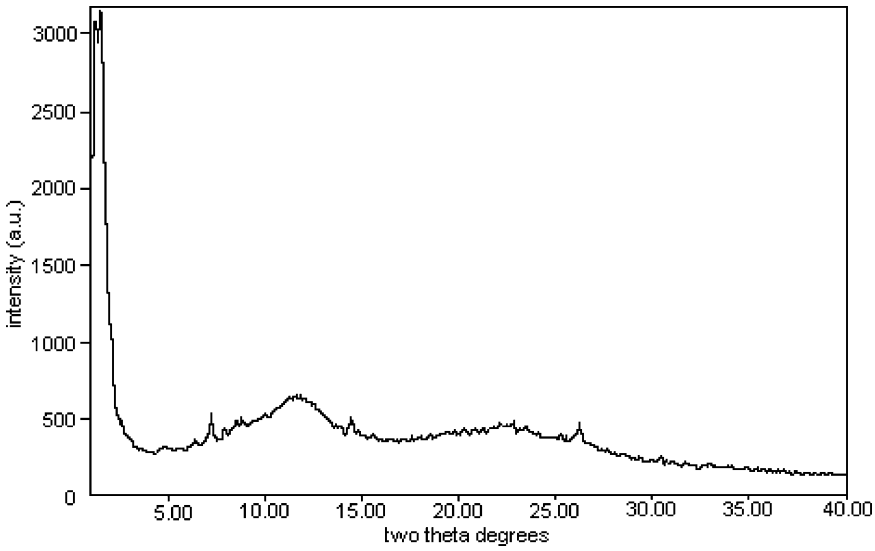

Fig. 5. Powder X-ray diffraction pattern of MCM-36.

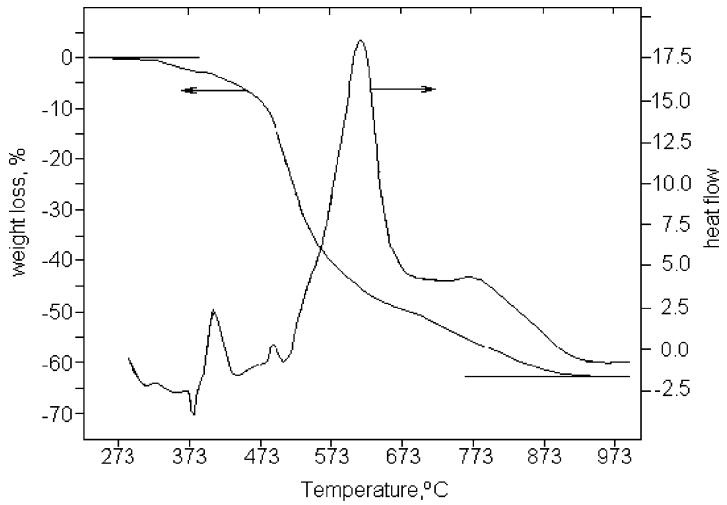

Fig. 6. TG and DTA profiles for MCM-36 samples.

advantage of being inexpensive and "gentle" towards the enzyme. This method profits from interactions between the support surface and the outer shell of the enzyme; the enzyme is immobilized onto the solid support by low energy binding forces, e.g. Van der Waals interactions, hydrophobic interactions, hydrogen bonds, ionic bonds. Thus, the enzymes can be simply retained on the surface of the support without forming covalent bonds between the enzyme and the support.

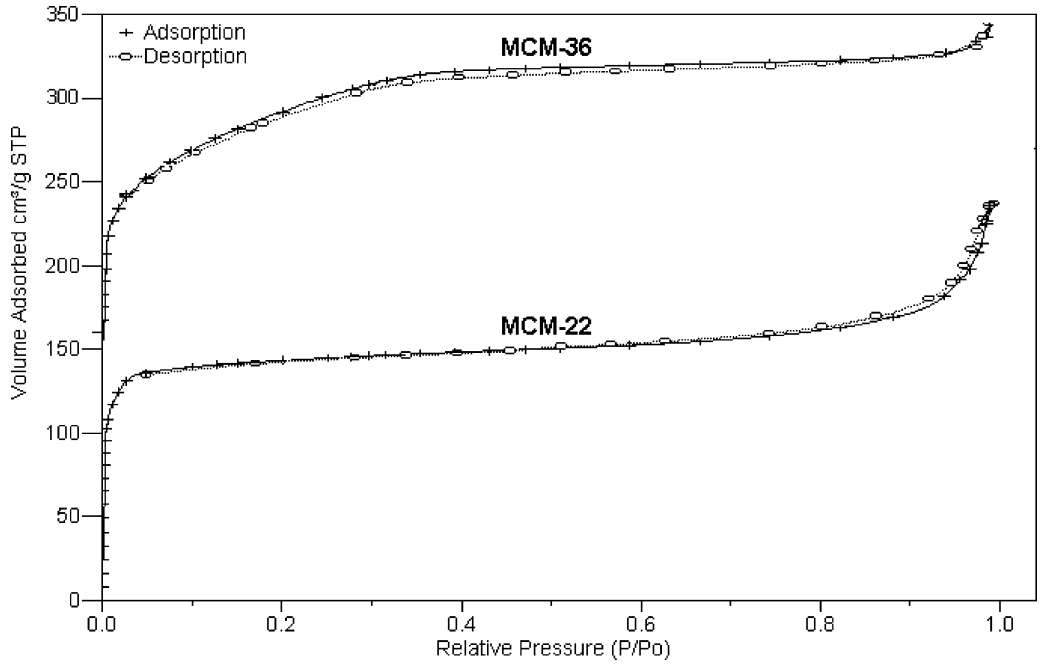

Fig. 7. N_2 isotherms of a MCM-22 and MCM-36 samples.

Table 1
Transesterification activity of CALB immobilized by physical adsorption on MCM-22 and MCM-36 zeolites

Sample	Adsorbed protein (mg/mg solid)	Transesterification rate (μmol/min × 10^{-2} per mg catalyst)	Transesterification rate (μmol/min per mg immobilized CALB)
MCM-22/pa	0.020	5.26	2.63
MCM-36/pa	0.004	3.59	8.98

It is of interest to note that lipases display a statistically significant enhanced occurrence of non-polar residues close to the surface, clustering around the active site [52]. Consequently, in contrast to the majority of enzymes, which preferably adsorb on materials which have polar surfaces, lipases are better adsorbed on hydrophobic carriers due to their peculiar physicochemical character.

When zeolites are used as support, the enzyme adsorption may occur only on the external surface. In the case of the mesoporous materials the adsorption inside the pores is possible if they have pores enough large to accommodate the molecules of enzyme.

CALB is a globular α/β type protein with approximate molecular dimensions of 3.0 nm × 4.0 nm × 5.0 nm, and relative mass of 33 273 Da [53]. Though its isoelectric point is 6.0 [54] we preferred to perform the immobilization on MCM-22 and MCM-36 supports by adsorption at pH of 7.0, which is indicated as optimum for a maximum activity. The results of this process are shown in Table 1.

Table 1 shows that at equilibrium, the MCM-22 zeolite retains a larger amount of enzyme (20 mg CALB/mg support) on its surface than the hybrid material MCM-36 (4 mg CALB/g support). We can also note that we have not reached the maximum loading capacity of the supports. For instance, if we take an average diameter of 3.5 μm and an average thickness of 0.075 μm for the disk-like crystallites of MCM-22, with density of 1.65 and an estimated roughness factor of 1.5, the support will have an external specific area of 24.3 m^2/g. Considering that CALB has an average spherical diameter of 39.15 Å, the surface occupied by lipase molecules (20 mg/g zeolite) is 19.17 m^2/g, therefore 78% from the external specific area is covered by lipase. In the case of MCM-36, if we take into account that its surface is 1.5 times larger than that of the MCM-22 zeolite, only 4 mg of lipase/mg was retained, so the enzyme loading is far from the maximum coverage.

We chose for comparison only the reports where the immobilization of enzymes has been carried out at equilibrium. In the case of the mesoporous material MCM-36, a good correlation with the results reported by Diaz and Balkus [31] was found. Thus, the protein loading on MCM-41 (pore size ∼40 Å) was 3.8–5.8 mg (cytochrome *c*)/g, 4.9 mg papain/g, and 3.8–4.7 mg trypsin/g support. The amount of immobilized enzyme increases with the pore size: 106–152 mg subtilisin/g MCM-41 (pore size 50–68 Å), but only 15–28 mg subtilisin/g SBA-15 (50–92 Å) [34]. The last example also reveals that the surface characteristics of mesoporous materials are critical for the adsorption of enzyme molecules. As regards the immobilization of lipase on microporous zeolites, the amount of enzyme immobilized on MCM-22 was higher than those reported for zeolite NaX (0.12 mg acid phosphatase/g [19]) or for zeolite Y (8.2 mg lipase/g [23]).

As expected, the catalytic activity of the MCM-22-based biocatalyst is higher than that of the pillared biocatalyst due to the higher amount of retained enzyme. However, concerning the specific activity of CALB, i.e. the transesterification rate per mg of immobilized enzyme on the surface, the biocatalyst based on MCM-36 support is 3.4-fold more active than the biocatalyst based on MCM-22 zeolite (Table 1). Perhaps the lipase macromolecules adsorbed on the surface of MCM-36 adopt a more favorable shape/conformation.

Moreover, MCM-36 proved to increase its specific activity, as function of the enzyme loading, better than the free lipase. Fig. 8 shows that the specific activity of MCM-36 biocatalyst for the transesterification of vinyl acetate with 1-octanol was higher than the equivalent amount of free enzyme. Though positive effects of the immobilization on the catalytic activity of lipase (for instance [7]) have been reported, in this case we believe that the differences mainly result from the methods of preparation of the two biocatalysts.

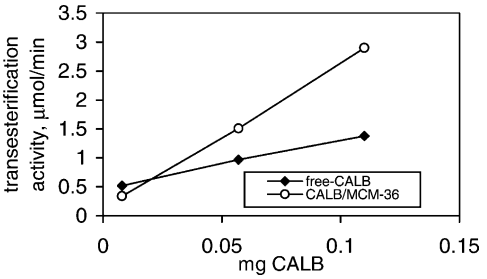

Fig. 8. Transesterification activity of MCM-36-immobilized (10 mg) and purified CALB with 1-octanol and vinyl acetate as acylating agent, in 1 ml of toluene at $T = 25\,^{\circ}C$.

The catalytic efficiency of biocatalyst particles will always depend on the exact method of preparation. Thus, Rees and Halling [54] proved that simple lyophilized powders often give substantially lower activity (per enzyme molecule) than the other forms. Two factors could be taken into the consideration: (i) the unfolding and inactivation due to the drying process [55], and (ii) the mass transfer limitation [54]. Studies on chemical modification of cutinase suspended in *n*-hexane by acyl chlorides and iodine [54] revealed that the rate of modification was always much faster for protein adsorbed to supports (silica or polypropylene) than for lyophilized powders. Consequently, it appears that access to most of the molecules in lyophilized powders involves a slow solid-state diffusion (which differs from the diffusion in pores). Solid-phase diffusion is not required for access to most support-adsorbed proteins, which is probably a major factor to their enhanced catalytic efficiency in organic media.

In order to verify these results we varied the amount of lipase retained on the surface of MCM-36 support. Since the enzyme is not soluble in an organic medium, it is possible to increase the amount of enzyme by simple deposition, as previously reported [20,24,25]. Several samples of supported enzyme were prepared as described in Section 2 in order to obtain various degrees of loading, from 0.625 to 15.5 mg enzyme/g support. These samples were tested as biocatalysts for the same acylation reaction (see Fig. 9).

The catalytic activity first increases with the amount of deposited enzyme; an optimum is reached at approximately 10 mg enzyme/g catalyst, and then it decreases. The decrease of activity can be explained by taking into account multi-layered stacking of enzyme molecules on the carrier surface, hence the internal layer of enzyme is less accessible for the substrate molecules [54,56]. The line reflecting the activity variation versus the amount of deposited enzyme reaches a plateau around of 2.5 mg lipase/g hybrid support and maximum at approximately 11 mg/g. Perhaps two "steps" occur in adsorption of enzymes on the heterogeneous surfaces: one operating at low, the other at higher enzyme concentrations [57]. As it was suggested [57], in the first step the enzyme adsorbs on the most favorable surfaces (here, the hydrophobic domains) in a fashion that enhanced its "unfolding" and therefore its activity. The second step would favor the formation of lipase "clusters" on the surface, analogous to the two-dimensional crystal proposed by

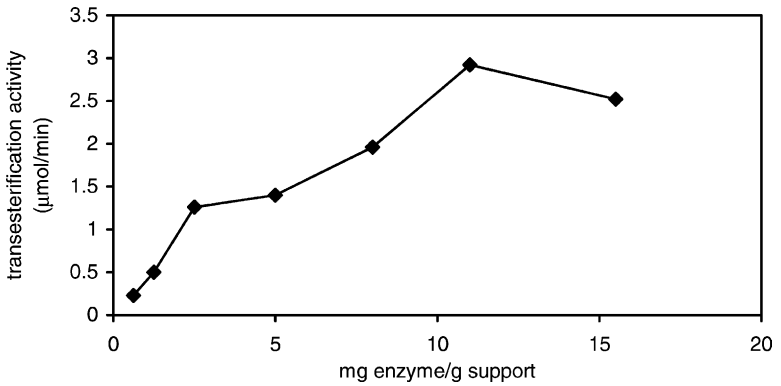

Fig. 9. Transesterification activity vs. the amount of enzyme loaded by deposition on MCM-36. The activities value were determined by the reaction of transesterification of vinyl acetate with 1-octanol in 1 ml toluene and using 10 mg of immobilized CALB; $T = 25\,^{\circ}C$.

Fair and Jamieson [58], thus resulting in an "apparent" increase in activity that does not well correlate with lipase loading (see also Fig. 9). This could be due to the unfavorable orientation or the activity is affected by the diffusion through the multi-layer lipase (deposit).

Note that a cluster could be formed before a monolayer coverage formation due to the existence of unfavorable surface regions (e.g. the hydrophilic environment, the abundance of water). Also, when the guest molecules are adsorbed inside the pores of the host matrix, part of the enzyme molecules, which deeply penetrated in the channels, could be blocked inside by the lately entered molecules.

Two different acylation reactions (the 1-octanol acylation by vinyl stearate and the 1-butanol acylation by vinyl acetate) were used to test the accessibility of substrates, with different bulkiness, to the enzyme molecules in the MCM-36 immobilized form, as well as in the lyophilized form (Table 2).

The data indicate that the diffusional limitations could play an important role. It should be noted that for both acylation reactions an increase of approximately 15 times for the amount of lyophilized enzyme leads to an increase of the catalytic activity of 2.2–3.3 times, whereas in the case of the immobilized enzyme an increase of only 9 times of the amount of deposited enzyme has as result an increase of 13–16 times of the catalytic activity. It is clear that the immobilization leads to a more advantageous use of the lipase, though a small difference between the activity ratios of the two systems of reaction was observed; this could be partially attributed to the difference of accessibility towards the active sites of immobilized enzymes that exists between the vinyl acetate/1-butanol and vinyl stearate/1-octanol acylation systems due to the different size of substrate molecules. In spite of this difference, the results confirm that in the immobilized form a facile access for the reactant molecules is assured, because the enzyme is highly dispersed on the surface of solid support. This is not the case of the multi-layered free enzyme.

Table 2
Transesterification activities of MCM-36-immobilized and free CALB for 1-butanol/vinyl acetate and 1-octanol/vinyl stearate reaction systems

Sample	Transesterification rate (μmol/min per mg catalyst)	Activity ratio
1-Butanol + vinyl acetate		
MCM-36 (0.012 mg)	0.042	16.3
MCM-36 (0.11 mg)	0.680	
Free CALB (0.011 mg)	0.92	2.2
Free CALB (0.158 mg)	2.04	
1-Octanol + vinyl stearate		
MCM-36 (0.012 mg)	0.043	13.1
MCM-36 (0.11 mg)	0.571	
Free CALB (0.011 mg)	0.32	3.3
Free CALB (0.158 mg)	1.05	

Of course, the most interesting questions are related to the mechanism of adsorption of the lipase molecules on the MCM-36 support and to the enhanced catalytic activity of the immobilized system. First, it is clear that the lipase molecules will be adsorbed through a combination of hydrophobic, Van der Waals and electrostatic forces, hydrogen bonds, etc. These interactions can be altered by solution conditions such as pH which make the adsorption process reversible.

As concerns the MCM-22 support, we chose a sample of zeolite with a silica to alumina ratio of 100. Because of its high Si/Al ratio it is assumed that the surface of zeolite has some regions with hydrophobic character, which will promote the adsorption of enzyme by hydrophobic forces. On the other hand, the substitution of aluminum atoms in the zeolite lattice generates negative charges in the framework, which can promote adsorption through electrostatic forces through positively charged lysine residues on the enzyme. At the same time, terminal silanols placed particularly around the mouth of pores can promote the adsorption through hydrogen bonding interactions with the enzyme. Therefore, it is reasonable to assume that the surface of MCM-22 support has both hydrophobic and hydrophilic properties. It seems that the hydrophobic feature of the zeolite is more important, since over 75% from its external surface is covered by lipase molecules.

By contrast, the pillaring process leading to MCM-36 will generate large domains with hydrophilic character; the gallery of pillars has large surfaces lined by silanols groups (Fig. 10). Thus, the adsorption of lipase mainly depends on the interactions of silanols from the mesoporous regions with hydrophilic (e.g. serine) residues of the enzyme. During CALB adsorption onto the hybrid support, a part of the lipase may be adsorbed onto the exterior,

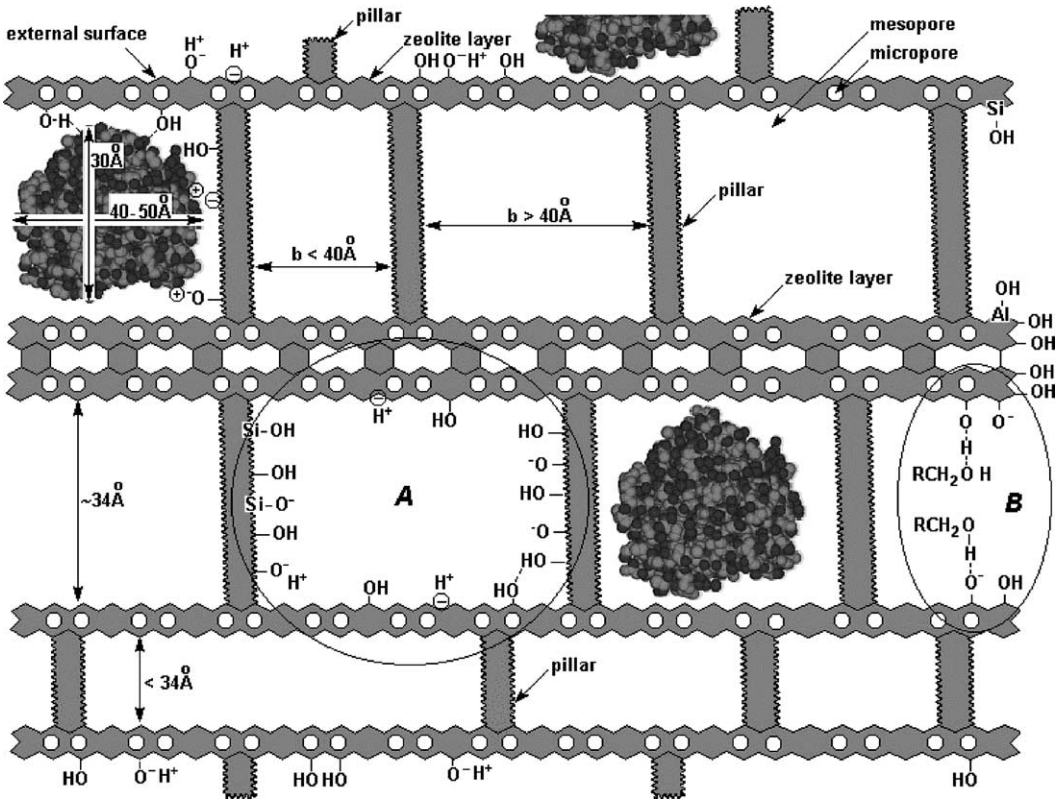

Fig. 10. Schematic presentation of the lipase adsorption on MCM-36.

perhaps at the entrance of pores, and part of enzyme molecules might be retained inside the mesopores of MCM-36. The presently available data do not allow a firm conclusion regarding the distribution of the enzyme over outer/inner surface.

As concerns the high catalytic activity of the MCM-36-based biocatalyst, the following hypothesis could be taken into consideration:

(i) the lipase molecules are highly dispersed on the surface of MCM-36 support, thus the protein–protein interactions are avoided and high flexibility is achieved;
(ii) the physical bonding inside the mesopores facilitates a favorable orientation of the lipase molecules toward the hydrophobic medium;
(iii) the silica rich domain behaves as a "reservoir" for the alcohol molecules; because of the non-polar solvent the alcohol molecules are oriented toward the polar surface to which they are bonded by hydrogen bonds (Fig. 10, medallion B). Thus, a high concentration of substrate is assured. Also, the alcohol molecules accumulated on the polar surface of mesopores could create a hydrophobic barrier by their alkyl chains between the carrier surface and the enzyme molecules and a more favorable reactional medium for lipase is generated.

The present results may encourage the application of MCM-36 molecular sieves as support for lipase immobilization. Though the loading capacity was relatively small, it could be improved optimizing the pillaring process. Also, further studies are required both in terms of adsorption protocol and of catalytic activity. Nevertheless, MCM-36-immobilized *Candida antarctica* B lipase seems to work well as suitable preparation for lipase applications.

4. Conclusions

MCM-36 was synthesized from pure MCM-22 precursor. With silica as pillaring material, the surface area of MCM-36 is about 1.5 times higher than that of MCM-22. Also, the resulting MCM-36 contains a mesoporous region between the microporous layers where the enzymes with suitable dimensions can be accommodated.

The physical immobilization of lipase on the mesostructure of MCM-36 has been demonstrated. Part of lipase molecules are assumed to be retained inside the mesopores of hybrid matrix. The loading capacity is comparable with that on other usual mesoporous supports like MCM-41. By comparison with MCM-22, the loading efficiency of the immobilized enzyme shows a clear correlation with the surface properties suggesting that certain zones of surfaces participate in the immobilization process. Catalytic tests indicate that MCM-36-immobilized enzyme is an active biocatalyst for the acylation reaction of alcohols, and its activity is higher than that of free lipase (at higher concentrations of enzyme).

References

[1] K.-E. Jaeger, M.T. Reetz, Trends Biotechnol. 16 (1998) 396.
[2] E.M. Anderson, M. Karin, O. Kirk, Biocatal. Biotransform. 16 (1998) 181.
[3] K. Drauz, H. Waldmann, Enzyme Catalysis in Organic Synthesis, vol. 1, VCH, Weinheim, 1995, p. 165.
[4] N.N. Gandhi, J. Am. Oil Chem. Soc. 74 (1997) 621.
[5] S.B. Petersen, in: F.X. Malcata (Ed.), Engineering of/with Lipases, Kluwer, Dordrecht, The Netherlands, 1996, p. 125.
[6] J.J. Lalonde, C. Govardhan, N. Khalaf, A.G. Martinez, K. Visuri, A.L. Margolin, J. Am. Chem. Soc. 117 (1995) 6845.
[7] M.T. Reetz, A. Zonta, J. Simpelkamp, Biotechnol. Bioeng. 49 (1996) 527.
[8] L. Cao, U.T. Bornscheuer, R.D. Schmid, J. Mol. Catal. B: Enzym. 6 (1999) 278.
[9] M.W. Baillargeon, P.E. Sonnet, J. Am. Oil Chem. Soc. 65 (1998) 1812.
[10] E. Katchalski-Katzir, D.M. Kraemer, J. Mol. Catal. B: Enzym. 10 (2000) 157.
[11] P.C. de Oliveira, G.M. Alves, H.F. de Castro, Biochem. Eng. J. 5 (2000) 63.
[12] J. Kroll, F.R. Hassanien, E. Glapinska, C. Franzke, Die Nahrung 24 (1980) 215.
[13] S. Hertzberg, L. Kvittingen, T. Anthosen, G. Skjak-Brack, Enzyme Microb. Technol. 14 (1992) 42.
[14] H.F. de Castro, P.C. Oliveira, G.M. Zanin, C.M.F. Soares, J. Am. Oil Chem. Soc. 76 (1999) 144.
[15] S.K. Khare, M. Nakajima, Food Chem. 68 (2000) 153.
[16] L. Cao, U.T. Bornscheuer, R.D. Schmid, J. Mol. Catal. B: Enzym. 6 (1999) 279.
[17] J.A. Bosley, J.C. Clayton, Biotechnol. Bioeng. 43 (1994) 934.
[18] E. Lie, G. Molin, J. Chem. Tech. Biotechnol. 50 (1991) 549.
[19] F. Alfani, L. Cantarella, M. Cantarella, A. Galifuoco, C. Colella, Stud. Surf. Sci. Catal. 84 (1994) 1115.
[20] A.P. Gonçalves, J.M. Lopes, F. Lemos, F. Ramôa Ribeiro, D.M.F. Prazeres, J.M.S. Cabral, M.R. Aires-Barros, J. Mol. Catal. B: Enzym. 1 (1996) 53.
[21] X.Z. Wang, T. Dou, Y.Z. Xiao, Prog. Chem. 9 (1997) 379.
[22] B. Liu, R. Hu, J. Deng, Anal. Chem. 69 (1997) 2343.
[23] Z. Knezevic, L. Mojovic, B. Adnajevic, Enzym. Microb. Technol. 22 (1998) 275.
[24] F.N. Serralha, J.M. Lopes, F. Lemos, D.M.F. Prazeres, M.R. Aires-Barros, J.M.S. Cabral, F. Ramôa Ribeiro, J. Mol. Catal. B: Enzym. 4 (1998) 303.
[25] G.-W. Xing, X.-W. Li, G.-L. Tian, Y.-H. Ye, Tetrahedron 56 (2000) 3517.
[26] F.N. Serralha, J.M. Lopes, L.F. Vieira Ferreira, F. Lemos, D.M.F. Prazeres, M.R. Aires-Barros, J.M.S. Cabral, F. Ramôa Ribeiro, Catal. Lett. 73 (2001) 63.
[27] F.N. Serralha, J.M. Lopes, M.R. Aires-Barros, D.M.F. Prazeres, J.M.S. Cabral, F. Lemos, F. Ramôa Ribeiro, Enzyme Microb. Technol. 31 (2002) 29.
[28] G. Saltharam, B.A. Saville, Enzyme Microb. Technol. 31 (2002) 747.
[29] P. Liu, Y.-H. Ye, G.-L. Tian, K.-S. Lee, M.-S. Wong, W.-H. Lo, Synthesis 6 (2002) 726.
[30] I.E. de Fuentes, C.A. Viseras, D. Ubiali, M. Terreni, A.R. Alcantara, J. Mol. Catal. B: Enzym. 11 (2001) 657.
[31] J.F. Diaz, K.J. Balkus Jr., J. Mol. Catal. B: Enzym. 2 (1996) 115.
[32] M.E. Gimon, V.L. Jimenez, L. Washmon, K.J. Balkus Jr., Stud. Surf. Sci. Catal. 117 (1998) 373.
[33] J. He, X. Li, D.G. Evans, X. Duan, C. Li, J. Mol. Catal. B: Enzym. 11 (2000) 45.
[34] H. Takahashi, B. Li, T. Sasaki, C. Miyazaki, T. Kajino, S. Inagaki, Micropor. Mesopor. Mater. 44–45 (2001) 755.
[35] L. Ren, J. He, D.G. Evans, X. Duan, R. Ma, J. Mol. Catal. B: Enzym. 16 (2001) 65.
[36] M. Kamori, T. Hori, Y. Yamashita, Y. Hirose, Y. Naoshima, J. Mol. Catal. B: Enzym. 9 (2000) 269.
[37] M.T. Reetz, A. Zonta, V. Vijayakrishnan, K. Schimossek, J. Mol. Catal. A: Chem. 134 (1998) 251.
[38] A.-F. Hsu, T.A. Foglia, S. Shen, Biotechnol. Appl. Biochem. 31 (2000) 179.
[39] S. Karlsson, S. Backlund, F. Eriksson, G. Hedström, Colloids Surf. B: Biointerface 10 (1998) 137.
[40] C.T. Kresge, W.J. Roth, K.G. Simmons, J.C. Vartuli, US Patent 5 229 341 (1993).
[41] A. Corma, C. Corell, J. Pérez Pariente, Zeolites 15 (1995) 2.
[42] A. Corma, V. Fornés, J. Martínez-Triguero, S.B. Pergher, J. Catal. 186 (1999) 57.
[43] F. Secundo, G. Carrea, D. Varinelli, C. Soregaroli, Biotechnol. Bioeng. 73 (2001) 157.

[44] M.K. Rubin, P. Chu, US Patent 4 954 325 (1990).
[45] M.E. Leonowicz, J.A. Lowton, S.L. Lawton, M.K. Rubin, Science 264 (1994) 1910.
[46] S.L. Lawton, M.E. Leonowicz, R.D. Partidge, P. Chu, M.K. Rubin, Micropor. Mesopor. Mater. 23 (1998) 109.
[47] S.L. Lawton, A.S. Fung, G.J. Kennedy, L.B. Alemany, C.D. Chang, G.H. Hatzikos, D.N. Lissy, M.K. Rubin, H.-K.C. Timken, S. Steuernagel, D.E. Woessner, J. Phys. Chem. 100 (1996) 3788.
[48] Y.J. He, G.S. Nivarthy, F. Eder, K. Seshan, J.A. Lercher, Micropor. Mesopor. Mater. 25 (1998) 207.
[49] G.J. Kennedy, S.L. Lawton, A.S. Fung, M.K. Rubin, S. Steuernagel, Catal. Today 49 (1999) 385.
[50] P. Mériaudeau, A. Tuel, T.T.H. Vu, Catal. Lett. 61(1999) 89.
[51] P. Wu, T. Komatsu, T. Yashima, Micropor. Mesopor. Mater. 22 (1998) 343.
[52] P. Fojan, P.H. Jonson, M.T.N. Petersen, S.B. Petersen, Biochimie 82 (2000) 1003.
[53] J. Uppenberg, M.T. Hansen, S. Patkar, T.A. Jones, Structure 2 (1994) 293.
[54] D.G. Rees, P.J. Halling, Enzyme Microb. Technol. 27 (2000) 549.
[55] A. Dong, S.J. Prestrelski, S.D. Allison, J.F. Carpenter, J. Pharm. Sci. 84 (1995) 415.
[56] R. Bovara, G. Carrea, G. Ottolina, S. Riva, Biotechnol. Lett. 15 (1993) 169.
[57] B. Al-Duri, Y.P. Yong, Biochem. Eng. J. 4 (2000) 207.
[58] B.D. Fair, A.M. Jamieson, J. Colloid Interface Sci. 77 (1980) 525.